# EVALUATION OF THE FATIGUE CRACK GROWTH OF AN ABNT 4133 MODIFIED STEEL (API - 5CT)[1]

Jefferson José Vilela[2]
Mariana Pimenta Alves[3]
José Rubens Gonçalves Carneiro[4]
Larissa Vilela Costa[5]
Marc Scibetta[6]
Raquel Maria Rocha Oliveira Menezes[7]
Geraldo de Paula Martins[8]

**Abstract**
The petroleum industry demand is impelling the development of steels with better resistance while keeping good resistance to fatigue crack growth. The objectives of this research are the fatigue crack growth and microstructure characterization of an ABNT 4133 modified steel (API 5CT) manufactured by continuous ingot casting. The generated experimental data in term of fatigue crack growth rate *versus* stress-intensity factor allows the validation of the Paris-Erdogan model in the stage II region and the Collipriest model down to the fatigue threshold up to the material fracture toughness.
**Key words:** Fatigue crack growth; ABNT 4133 steel; API 5CT.

## ANÁLISE DO CRESCIMENTO DE TRINCA POR FADIGA DO AÇO ABNT 4133 MODIFICADO (API 5CT)

**Resumo**
A demanda da indústria petrolífera tem impulsionado o desenvolvimento de aços com resistência à fadiga em meios corrosivos. Os objetivos deste trabalho foram a determinação de expressões matemáticas para a taxa de propagação de trinca por fadiga *versus* a faixa do fator de intensidade de tensão, em amostras do aço ABNT 4133 modificado (API 5CT) obtidas por lingotamento contínuo e a análise da influência da microestrutura. O modelo de Paris-Erdogan foi aplicado ao estágio II da propagação e os resultados estão de acordo com outros pesquisadores. O modelo de Collipriest aplica-se a toda a curva e é influenciado pelo $\Delta K_{th}$ (faixa limiar de fator de intensidade de tensão) e $K_c$ (tenacidade à fratura) do material.
**Palavras-chave:** Crescimento de trinca por fadiga; Aço ABNT 4133 e API 5CT.

# 1 INTRODUCTION

Brazil energy policy is striving for the self-sufficiency of oil and derivatives. Moreover, the prices instability is a driving force for the activities of exploration and production. High strength steel specified according to standard API (American Petroleum Institute) has been developed for the Brazilians steel plants once the exploration of oil in Brazil shows new challenges as a consequence of the depth where the reserves are found. Amongst these challenges, the presence of carbonic gas ($CO_2$) and acid hydro-sulfuric ($H_2S$), the latest being extremely corrosive and dangerous for the tubing, mainly in the covering of the oil wells. The concentration of $H_2S$ in the oil or gas, associated to the pH level of the environment, is determinant for corrosion. Metallic structures such as a column of oil exploration in a corrosive environment of $H_2S$ can have its life drastically reduced due to stress corrosion.

Recent improvement of the mechanical resistance of structural steels increases safety of the components. Generally, these types of steel are stabilized with titanium, which combines with free nitrogen to the expense of fracture toughness degradation. To compensate the decrease of mechanical resistance due to lower carbon, concentration of titanium and vanadium are raised and cause intense refining of grain in conjunction with Niobium besides the development of acicular ferrite.[1] A thermomechanical processing at temperatures higher than usual is adopted because the Niobium increases the temperature of no-recrystallization ($T_{nr}$), which allows lower loads of rolling and the material with a good toughness.

The structural steel must have a good weldability and the mechanical properties of the joint must be similar or better than the base metal. Amongst these mechanical properties, are the tensile strength, toughness fracture and the resistance to fatigue crack growth.[2] The objective of the present work is to study the fatigue properties of crack growth for ABNT 4133 modified steel (API 5CT).[3]

Fatigue can be defined as a phenomenon that occurs in components and structures submitted to cyclical external loadings and it manifests through the deterioration of the material ability to tolerate the loading that it was projected to sustain.[4] Therefore, it is important to identify the fatigue crack growth mechanism, with the objective of improving the characteristics of the material.

For the largest part of engineering alloys, the curve $\log(da/dN)$ ($a$: crack size, $N$: number of cycles) *versus* $\log(\Delta K)$ ($\Delta K$: stress intensity factor range) exhibits a sigmoidal variation, divided in stages I, II and III,[5] whose characteristics are:

• Stage I – the crack and the plastic deformation which surround the crack tip are confined to a few grains; the crack growth occur predominantly by unique shearing on the direction of the primary sliding system; the medium increment by cycle is smaller than the space lattice and it is associate to $\Delta K_{th}$, below which crack growth doesn't occur. In practical terms, $\Delta K_{th}$ is defined as the stress intensity factor range, whose crack growth rate is equal to $10^{-7}$ mm/cycle.

• Stage II – it occurs in ranges of higher stress intensity value; the plastic zone in the crack tip incorporates many grains; crack growth process involves flow through two sliding systems; the crack growth through the progress of a fixed quantity by stress cycle; the microstructure and the loading conditions aren't very important at this stage.

• Stage III – it corresponds to the final abrupt fracture that occurs in the last stress cycles, when the crack, which has developed in a progressive way, reaches a critical size for unstable propagation and catastrophic failure; it suffers a great influence of microstructure and loading conditions.

For the constant loading amplitude, different models predicted the fatigue crack propagation. They involve material constants, loading rates and operating stress level. The Paris-Erdogan model[6] (Eq. 1) is a simple empiric relation that obeys a power equation and describes the fatigue crack growth in the stage II of the curve *da/dN versus ΔK*, in which *C* and *m* are material constants that are experimentally determined.

$$\frac{da}{dN} = C \cdot \Delta K^m \qquad (1)$$

The Paris-Erdogan model is unable to model the fatigue propagation rate for low levels of *ΔK*, in stage I. The biggest part of fatigue life occurs at this stage. The model of Paris and Erdogan models the crack propagation in stage II and later the propagation occurs instantly.
Collipriest model[7] is represented by Equations 2, 3 and 4 and it is valid for the three regions I, II e III:

$$log\frac{da}{dN} = C_1 + C_2 \cdot tanh^{-1}\left[\frac{log\left(\frac{\Delta K^2}{\Delta K_{th} \cdot K_c \cdot (1-R)}\right)}{log\left(\frac{K_c \cdot (1-R)}{\Delta K_{th}}\right)}\right] \qquad (2)$$

$$C_1 = log\left(C \cdot \left(K_c \cdot \Delta K_{th}\right)^{n/2}\right) \qquad (3) \qquad\qquad C_2 = log\left(\frac{K_c}{\Delta K_{th}}\right)^{n/2} \qquad (4)$$

R is the stress ratio (with stress ratios less than zero set equal to 0),
$K_c$ is the material fracture toughness,
$\Delta K_{th}$ is the threshold fatigue crack growth.

$C_1$ and $C_2$ are the parameters that represent, respectively, the offset of the abscissa axis and the slope of the curve, when it cuts the abscissa axis.
This curve is asymptotic to the abscissa *(1 − R)K_c* and *(1 − R)K_{th}*. This model describes the fatigue crack propagation in the three areas, it means, from threshold *ΔK_{th}* (stage I) to the critical amplitude of fracture toughness *ΔK_c = (1 − R)K_c* (stage III), but it requires the determination of *K_c* and *ΔK_{th}* experimentally in addition to the C and n material constants.

## 2 MATERIAL AND METHODS

The material used in this study was ABNT 4133 modified steel (API 5CT) supplied in the continuous ingot casting by Vallourec & Mannesmann Tubes – V&M S/A in disks with diameter of 230 mm and thickness of 20 mm and its composition is shown in Table 1. Metallograpy was done with a 2% Nital solution.

**Table 1** – Chemical composition of ABNT 4133 modified steel (API 5CT) (in weight percent).

| C | Mn | P | S | Si | Ni | Cr | Mo | Al | V | Nb | Ti | Cu | Sn |
|---|---|---|---|---|---|---|---|---|---|---|---|---|---|
| 0.33 | 0.46 | 0.012 | 0.002 | 0.29 | 0.01 | 0.95 | 0.78 | 0.031 | 0.043 | 0.028 | 0.012 | 0.03 | 0.001 |

Source: Valourec & Mannesmann Tubes – V&M S/A.

The mechanical properties of the material at room temperature were obtained from tension tests using shouldered-end specimens in accordance with standard ASTM E8M[8] and the test's velocity adopted was 2,0 mm/min. An electromechanical Instron machine, model TTDML, with load cell capacity of 100 kN was used for testing.

Fatigue crack growth rate (FCGR) tests were carried out on a servo hydraulic Instron testing machine with a 250 kN capacity, model 8802, with computer interface, load and position control and data acquisition. The crack size measurement was done by compliance measurement using an Instron clip-gage, model 2670-122, with opening from 10 to 6 mm. Pre-cracked C(T) specimens with thickness $B$ = 14 mm and width $W$ = 60 mm were used under constant $\varDelta K$ in three stages with $\Delta a$ = 1 mm: $1^{st}$ – 20 MPam$^{1/2}$, $2^{nd}$ – 18 MPa m$^{1/2}$ and $3^{rd}$ – 16 MPa m$^{1/2}$, according to methodology developed by *Reis et al*[9] and ASTM E647 [10], with stress ratio value of 0.1 The tests were conduced at room temperature with at constant load amplitude of 10.8 kN at a frequency of 20 Hz and stress ratio value of 0.1, according Table 2. The specimens were machined in the C-R orientation. Dimensions of C(T) specimens are shown in Figure 1.

**Table 2** – Number of fracture mechanical tests specimens.

| Type of test | $K_c$ | *da/dn:* constant amplitude load | *da/dn:* $\Delta K$ decreasing |
|---|---|---|---|
| Type of specimen | 1 SENB | 3 CT | 1 CT |

Fracture analyses were made on broken test specimens using a Scanning Electron Microscope Phillips with EDS, electric potential 20 kV and magnify 50 to 800 X.

For the Collipriest[7] model, it was also necessary to evaluate the fatigue crack growth threshold ($\varDelta K_{th}$) and the fracture toughness ($K_c$) of the material. The $\varDelta K_{th}$ parameter was obtained through the method proposed in standard ASTM E647,[10] in which the stress intensity factor range ($\varDelta K$) is gradually reduced until the fatigue crack growth rate (*da/dN*) reaches the prescribed value of $10^{-7}$ mm/cycle. This test was performed at room temperature, once again through C(T) specimens, using a normalized K-gradient value defined by the standard.

The $K_c$ parameter was obtained according to ASTM E399[11] in the same equipment used for FCGR and $\varDelta K_{th}$ tests, at room temperature. For this test a SENB specimen with width $W$ = 18 mm and thickness $B$ = 18 mm was used, at room temperature. A software from Instron controlled the machine during the test. The final crack length was measured optically and $K_Q$ (provisory material fracture toughness) was calculated.
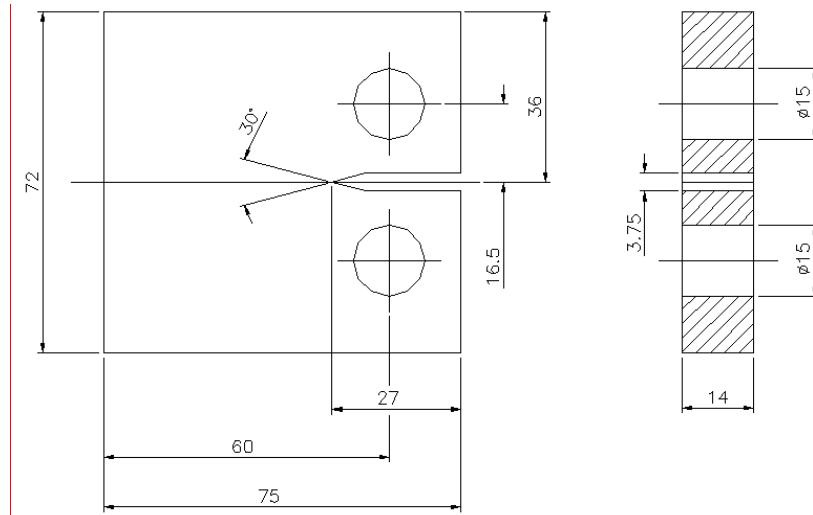
**Figure 1** – Dimensions (mm) of C(T) specimens for fatigue crack growth tests.

## 3 RESULTS

The average values for mechanical properties obtained by two tensile tests specimens at room temperature are showed in Table 3, in which $\sigma_{YT}$ is the yield tensile strength, $\sigma_{UT}$ the ultimate tensile strength, $\xi$ the total elongation and $A$ the reduction of area.[3]

**Table 3** – Room temperature mechanical properties of ABNT 4133 modified (API 5CT) steel manufactured by continuous ingot casting.

| $\sigma_{YT}$ [MPa] | $\sigma_{UT}$ [MPa] | $\xi$ [%] | A [%] |
|---|---|---|---|
| 778 ± 11 | 920 ± 16 | 3.5 ± 0.7 | 4.0 ± 0.7 |

Figure 2 shows the gross structure of ABNT 4133 modified steel (API 5CT) manufactured by continuous ingot casting. It was heterogeneous and possibly formed by ferrite and bainite. For a more specific determination, X-ray tests would be necessary.

The fractography of a tensile specimen showed dimples near porosity area (Figure 3a) and macles starting from internal cracks (Figure 3b). In Figures 3c and 3d, the macles appear from macro-inclusion, whose composition determined by EDS analysis showed the presence of calcium and magnesium carbonate (Figure 4). The tensile fracture was brittle due to macle from microporosity and internal micro cracks.

A fracture surface analysis of a fatigue C(T) specimen was made. The analysis concentrate on the beginning of the fatigue crack and final crack propagation region. Nucleation area showed narrow grooves that change their direction when microcracks are found (Figure 5a). There were macles in the beginning of the fatigue crack and propagation region (Figure 5b), as well as dendrites of solidification (Figure 5c). The rupture region showed a brittle behavior (Figure 5d).
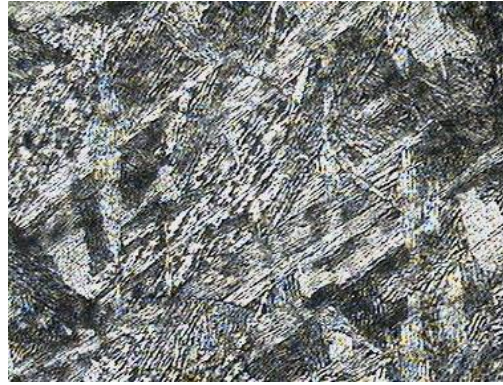
**Figure 2** – Microstructure of ABNT 4133 modified steel (API 5CT) manufactured by continuous ingot casting. The scale of magnification was 200X.



**(a)** **(b)**



**(c)** **(d)**
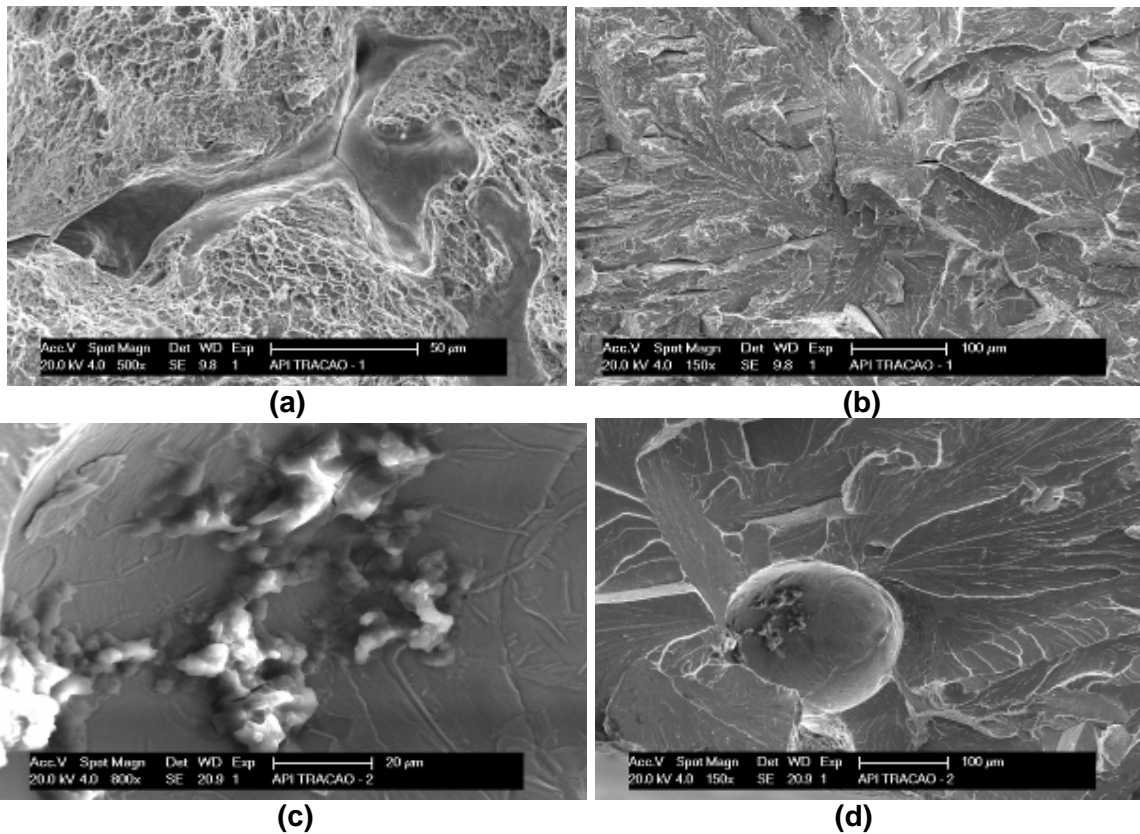
**Figure 3** – Fractography of a tensile specimen of ABNT 4133 modified steel (API 5CT) manufactured by continuous ingot casting at a Scanning Electron Microscope (SEM).
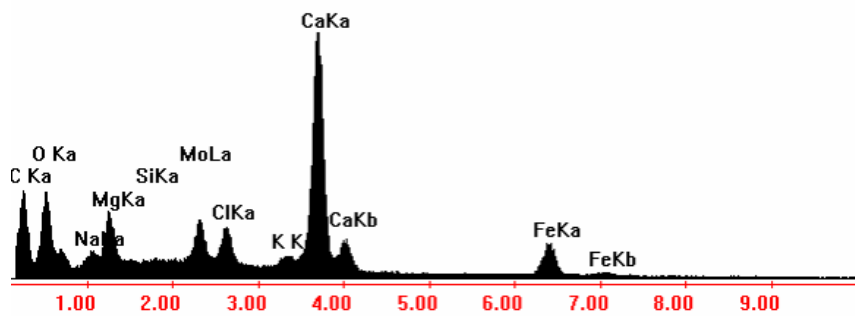


**Figure 4** - EDS analysis for a macro-inclusion of ABNT 4133 modified steel (API 5CT) ) manufactured by continuous ingot casting.
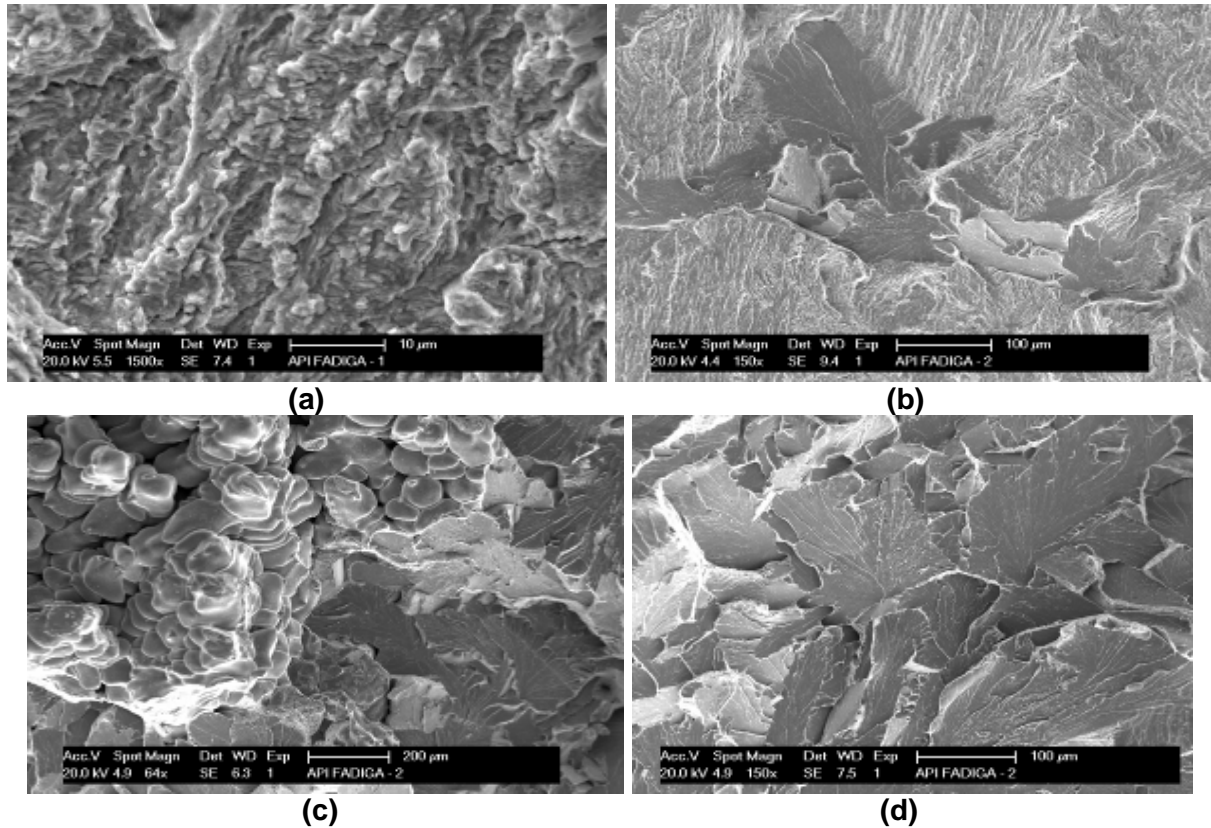
**Figure 5** – Fractography of a fatigue specimen of ABNT 4133 modified steel (API 5CT) at a Scanning Electron Microscope (SEM).

Fatigue crack growth rate in function of stress intensity factor range curves were obtained for three specimens at room temperature (Figure 6). The Paris-Erdogan model was applied to stage II and the values obtained for its coefficient *C* and exponent *m,* as well as the statistic coefficient of determination $R^2$, are shown in Table 4.
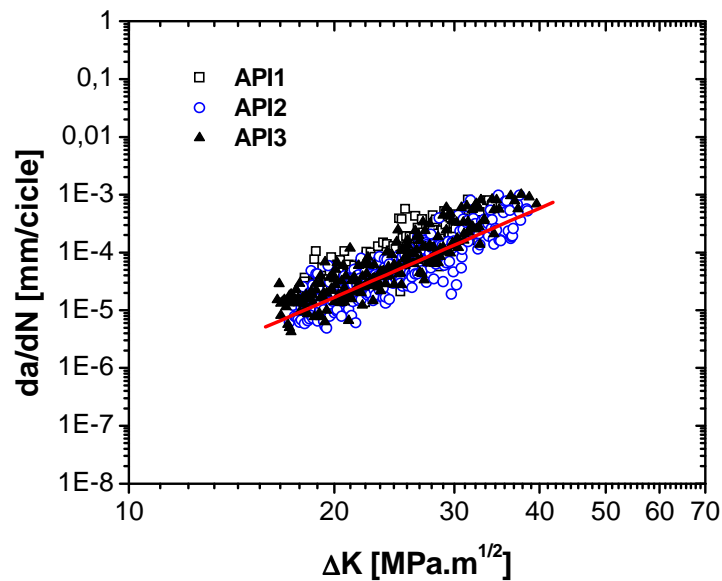


**Figure 6** – Paris-Erdogan model for *da/dN x ΔK* curves of ABNT 4133 modified steel (API 5CT) manufactured by continuous ingot casting. Tests under *f* = 20Hz and *R* = 0.1, specimens with *B* = 14 mm and C-R direction.

**Table 4** – Parameters of Paris-Erdogan model for *da/dN x ΔK* curves of ABNT 4133 modified steel (API 5CT) manufactured by continuous ingot casting. Tests under $f$ = 20Hz and $R$ = 0.1, specimens with $B$ = 14 mm and C-R direction.

| | C | m | $R^2$ |
|---|---|---|---|
| API1 | $1.99 \times 10^{-12}$ | 5.42 | 0.793 |
| API2 | $3.72 \times 10^{-12}$ | 5.12 | 0.790 |
| API3 | $3.23 \times 10^{-12}$ | 5.34 | 0.725 |

Prior the identification of the Collipriest[7] model, the values for the fatigue threshold and fracture toughness given in Table 5 were obtained.

**Table 5** – Fatigue threshold and fracture toughness values of ABNT 4133 modified steel (API 5CT) manufactured by continuous ingot casting.

| | |
|---|---|
| $\Delta K_{th}$ [MPa.m$^{1/2}$] | 9.43 |
| $K_Q$ [MPa.m$^{1/2}$] | 80.6 |

The Collipriest[7] model was then applied to the whole *da/dN* versus *ΔK* curve as shown in Figure 7. Table 6 contains the values obtained by fitting for parameters $C$ and $n$ and $R^2$.
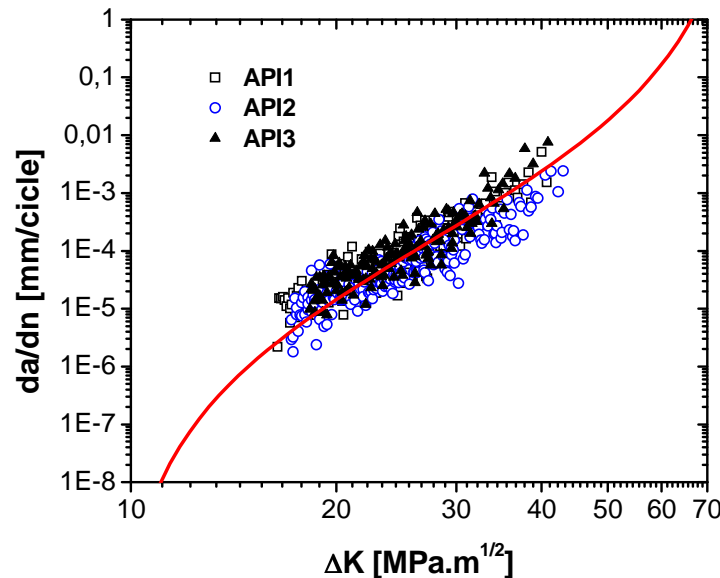


**Figure 7** – Collipriest[7] model for *da/dN x ΔK* curves of ABNT 4133 modified steel (API 5CT) manufactured by continuous ingot casting. Tests under $f$ = 20 Hz and $R$ = 0.1, specimens with $B$ = 14 mm and C-R direction.

**Table 6** – Parameters of Collipriest model for *da/dN x ΔK* curves of ABNT 4133 modified steel (API 5CT) manufactured by continuous ingot casting. Tests under $f$ = 20Hz and $R$ = 0.1, specimens with $B$ = 14 mm and C-R direction.

| C | n | $R^2$ |
|---|---|---|
| $4.11 \times 10^{-7}$ | 1.78 | 0.684 |
| $1.84 \times 10^{-6}$ | 1.27 | 0.494 |
| $1.11 \times 10^{-7}$ | 2.20 | 0.846 |

## 4 DISCUSSIONS

The Paris-Erdogan modeling of *da/dN versus ΔK* curves showed good agreement between the results of the three specimens as seen in Figure 6 and Table 4, although the dispersion given by $R^2$ is high. For tests on less brittle and more

homogeneous materials using the same equipment $R^2$ reaches values superior to 0.9. [12] The present dispersion could be caused by the microstructure employed, the steel had porosity and macro inclusion that create cleavage twin.

The FCGR parameters obtained by the Paris-Erdogan model are closer to those reached by Alves et al[13] and Miqueri[14] for the welded zone of low carbon steel. The high value of exponent $m$ shows that the fragility of the material causes a fast crack propagation.

References in the open literature for similar materials for the Collipriest model were not found. However, the results are consistent and the quality of the data fitting is similar to the Paris model. The reference for this analysis was found in Martins[12].

The value of the coefficient $C_2$ represents the curve's slope when it intercepts the abscissa. A lower $C_2$ means a flatter curve and a lower value of $n$, according to Martins[2]. So the values obtained for the model's parameters are consistent with the material properties.

## 5 CONCLUSIONS

The FCG of the ABNT 4133 modified steel (API 5CT) manufactured by continuous ingot casting had similar behavior of weld join in low carbon steel. Both the Paris-Erdogan and the Collipriest model were able to model properly the FCGR data in their domain of applicability.

No FCGR data on similar material could be found in the open literature.

Microstructure investigations provide some qualitative explanation for the relative high observed FCGR. The ABNT 4133 modified steel (API 5CT) manufactured by continuous ingot casting has behavior fragile due to flaws.

## REFERENCES

1 SICILIANO, F., Materiais para gasodutos: Aços de alta resistência para dutos de transporte de gás e petróleo - tendências atuais. *Metalurgia & Materiais*, São Paulo SP, v. 64, maio 2008, p. 208-211.
2 HIPPERT JÚNIOR, E. Investigação Experimental do Comportamento Dúctil de Aços API-X70 e Aplicação de Curvas de Resistência J- a para Previsão de Colapso em Dutos. São Paulo: USP, 2004. 167p. Tese (Doutorado em Engenharia Naval e Oceânica) - Escola de Politécnica da USP, 2004.
3 VALLOUREC & MANNESMANN TUBES, VAM Riser, site: http://www.vamservices.com/Library/files/Leaflet_VAM_RISER.pdf, accessed: 04/13/2004.
4 SURESH, S., *Fatigue of Materials*, Cambridge University Press, 1988.
5 ANDERSON, T. L., *Fracture Mechanics - Fundamentals and Aplications*, CRC Press, second edition, 2005.
6 PARIS, P.C.; ERDOGAN, F. A Critical Analysis of Crack Propagation Laws. *Journal of Basic Engineering 85*, 1963. p. 528-534.

7    COLLIPRIEST, J. E., "An Experimentalist's View of the Surface Flaw Problem", The Surface Crack: Physical Problems and Computational Solutions, ASME, 1972, pp. 43-62.

8    AMERICAN SOCIETY FOR TESTING AND MATERIALS. E 8M, *Standard Test Methods for Tension Testing of Metallic Materials*. Philadelphia: ASTM, 2005.

9    REIS, E.; ALVES, M. P.; VILELA, J. J. *Ensaios de Propagação de Trinca por Fadiga: Rotina interna do Laboratório de Ensaios Mecânicos do CDTN/CNEN*, LABMEC/006, Belo Horizonte, 2009.

10   AMERICAN SOCIETY FOR TESTING AND MATERIALS. E 647-99. *Standard Test Method for Measurement of Fatigue Crack Growth Rates*. Philadelphia: ASTM, 2005.

11   AMERICAN SOCIETY FOR TESTING AND MATERIALS. E 399-90. *Standard Test Method for Plan-Strain Fracture Toughness of Metallic Materials*. Philadelphia: ASTM, 2005.

12   MARTINS, G. P. *Tenacidade a Fratura e Propagação de Trinca em Juntas Soldadas de Aço Estrutural Resistente a Corrosão Atmosférica*. Thesis (Ph.D .in Mechanical Engineering) - Universidade Federal de Minas Gerais. Belo Horizonte: UFMG, 2004.

13   ALVES, M. P.; VILELA, J. J.; MARTINS, G. P.; CARNEIRO, J. R. G.; COSTA, L. V.; CAMPOS, W. R. C.; LEITÃO, C. E. Modelagem da Propagação de Trinca por Fadiga de Juntas do Aço ABNT 1016 Soldadas por Processo GMAW. In: V Congresso Brasileiro de Engenharia de Fabricação, Belo Horizonte, 2009.

14   MIQUERI, F. R. *Comportamento do crescimento de trinca por fadiga de um aço ABNT 1016 laminado a quente e soldado por MAG*. Dissertation (Master in Mechanical Engineering) – Mechanical Engineering Department from PUC Minas. Belo Horizonte: PUC Minas, 2006.